International Journal of Lightweight Materials and Manufacture 3 (2020) 77–87

Contents lists available at ScienceDirect

International Journal of Lightweight Materials and Manufacture

journal homepage: https://www.sciencedirect.com/journal/international-journal-of-lightweight-materials-and-manufacture

Original Article

Experimental investigations on the effects of projectile hardness on the impact response of fibre-reinforced composite laminates

Haibao Liu [a], Jun Liu [a], Cihan Kaboglu [a], Hui Chai [b], Xiangshao Kong [c], Bamber R.K. Blackman [a], Anthony J. Kinloch [a], John P. Dear [a, *]

[a] Department of Mechanical Engineering, Imperial College London, South Kensington Campus, London SW7 2AZ, UK
[b] AVIC The First Aircraft Institute, Xi'an, Shaanxi 710089, People's Republic of China
[c] Departments of Naval Architecture, Ocean and Structural Engineering, School of Transportation, Wuhan University of Technology, Wuhan, Hubei 430063, People's Republic of China

ARTICLE INFO

Article history:
Received 16 August 2019
Received in revised form
4 October 2019
Accepted 8 October 2019
Available online 18 October 2019

Keywords:
Soft impact
Projectile hardness
Digital Image Correlation
Damage mechanisms
Composites

ABSTRACT

This paper presents a detailed experimental investigation on the effects of projectile hardness on the behaviour of thermoplastic composites under impact loading. In this research, gas-gun experiments employ gelatine and high-density polyethylene (HDPE) projectiles, of the same mass and diameter, to impact against woven carbon-fibre reinforced poly (ether-ether ketone) (CF/PEEK) composite specimens. During the experiments, a high-speed camera is employed to capture the deformation of the projectiles and a three-dimensional (3D) Digital Image Correlation (DIC) system is employed to record the major strain and out-of-plane displacement of the thermoplastic composite specimens. Experimental results, including the Digital Image Correlation (DIC) output and the post-impact status, are obtained and compared to show the effects of harder projectiles on increasing the impact damage. The composite specimens, impacted by gelatine and high-density polyethylene (HDPE) projectiles, presented similar values of the major strain and out-of-plane displacement, but the high-density polyethylene (HDPE)-impacted composite specimens show more severe damage than the gelatine-impacted composite specimens.

1. Introduction

With their increasing application in the aircraft industry, polymer-matrix fibre-reinforced composite materials have attracted much attention from both academia and industry [1–3]. On the basis of an appropriate lay-up, such composites can possess excellent in-plane properties. However, composite laminates are very vulnerable to through-thickness impact loading [4–9], which can lead to a significant reduction of their structural strength. This drawback has considerably restricted the application of composite materials in main load-bearing structures. A better understanding of the impact behaviour of composite materials subjected to impact loading, especially by different types of projectiles, would contribute to the design and maintenance of composite structures. With this in mind, the focus of this paper is to investigate the behaviour of composite laminates subjected to impact loading by projectiles with different hardness.

Hou and Ruiz [10] investigated the impact resistance of composites subjected to high-velocity, soft-body impact loading. In their study, the soft-body projectile was made by mixing one part of bovine-hide gelatine with four parts of water. Impact experiments were performed at different energy levels by varying the velocity of the projectiles. Each panel was impacted only once and was then inspected using an ultrasonic C-scan system. The damage present in the various types of composites was identified and the impact resistance of these laminates was ranked based on the experimental results.

Zhou et al. [11] employed two different types of soft projectiles, prepared using gelatine and rubber, to perform the gas-gun impact on typical aircraft structures, e.g. monolithic aluminium alloy plates and laminated glass plates. During the experiments, the full field

* Corresponding author.
E-mail address: j.dear@imperial.ac.uk (J.P. Dear).
Peer review under responsibility of Editorial Board of International Journal of Lightweight Materials and Manufacture.

https://doi.org/10.1016/j.ijlmm.2019.10.001

out of plane displacements of the targets were recorded for velocities 110–170 m.s^{-1} using Digital Image Correlation. The results showed that, for the same kinetic energy, even though the out of plane displacements and in-plane strains, obtained from the composite specimens impacted by these two types of projectiles, were similar, the rubber projectile could exert a higher pressure on a target as compared to gelatine, which subsequently led to fractures in the impacted laminated glass plates.

Kim and Kedward [12] conducted experimental investigations on the response of composite laminates under hailstone impact. During the experiments, the ice balls were launched at a velocity range of 30–200 m.s^{-1} to impact onto composite panels. Based on the experimental results, the different failure modes and elastic responses exhibited by thin composite panels over a range of impact velocities were observed. Moreover, the lowest impact energy to initiate damage in the composite panels was assessed. Experimental results showed that a progressive failure existed in the composites, which started with delamination as the initial failure mode.

Although, many experimental and numerical studies have been conducted on the response of composite laminates under impact loading, there is less research on the effects of projectile hardness on the impact behaviour of composite laminates. In the present research, experimental studies on the impact behaviour of composites subjected to soft and hard projectiles are presented. In the experiments, soft gelatine projectiles and hard high-density polyethylene (HDPE) projectiles were employed to strike the composite target specimens. A high-speed camera was employed to capture the deformation and flow of the gelatine projectiles during the test and the deformations undergone by the composite specimens were recorded using a three-dimensional (3D) Digital Image Correlation (DIC) system. Both visual inspection and ultrasonic scan were conducted on the post-impact composite specimens to evaluate the impact damage. The experimental results extracted from the gelatine-impacted CF/PEEK and HDPE-impacted CF/PEEK composites were employed to investigate the effects of the projectile hardness on the impact behaviour of composites laminates.

2. Projectiles and composite specimens

2.1. The projectiles

To investigate the effects of the hardness of the projectile on the impact response of the composites, gelatine projectiles and HDPE projectiles, of the same mass, were prepared for the gas-gun impact experiments. The gelatine projectiles were prepared using a mixture of 10% by weight gelatine powder and 90% by weight distilled water. The gelatine powder was supplied by Honeywell Specialty, Germany. The HDPE projectiles were machined from HDPE rod, 'RS PRO Black' supplied by RS Components, UK. Fig. 1 shows the photographs of the typical gelatine and HDPE projectiles.

The gelatine projectiles had a nominal diameter of 23 mm and a nominal length of 45 mm. To produce a similar mass to the gelatine projectiles, the HDPE projectiles had the same nominal diameter of 23 mm but a slightly larger nominal length of 50 mm. The geometry and some key properties of the prepared projectiles are given in Fig. 2 and Table 1 [13–15].

2.2. Composite specimens

A woven T300 carbon fibre reinforced PEEK composite was evaluated. The woven carbon fibre ply possessed architecture of [0-90°]. These materials were supplied by Haufler Composites, Germany. An Out-of-Autoclave (OOA) manufacturing route was employed to consolidate the CF/PEEK prepregs. Diagrams of the consolidation jig and the cure schedule for the CF/PEEK prepregs are shown in Fig. 3a,b, respectively.

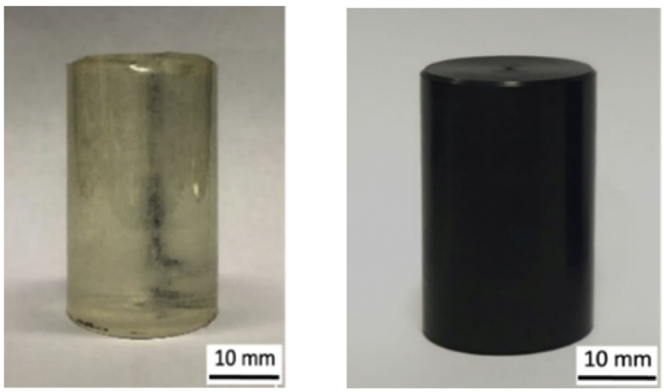

Fig. 1. The typical soft gelatine (left) and hard HDPE (right) projectiles.

Composite target test specimens were manufactured from the composite panels, see Fig. 4, using a diamond saw and a floor-standing drill. The lay-up employed for the CF/PEEK composite specimen was $[0\text{-}90^\circ]_{4s}$ and the nominal thickness of the manufactured specimens was 2 mm. The geometry of the composite target test specimens for the impact tests is given in Fig. 4a, and a specimen with a rear-face speckled pattern is illustrated in Fig. 4b.

Table 2 gives all the dimensions of the specimens, where H and W are the specimen height and width, respectively, when mounted in the support fixture. The length, d_3, defines the size of the DIC pattern area. The length, d_1, defines the distance between the sample edge and the centre line of the holes and d_2 defines the distance between each of the holes. The radius of each hole is R. For the DIC measurements, the specimens were first painted on the rear-face using a white matt paint and then 'speckled' using a paintbrush to form the matt-black pattern for the DIC measurements.

3. Experimental set-up

A helium-propellant gas-gun, which has a four-litre pressure vessel and a three-metre-long barrel, was employed to accelerate the projectiles in the impact tests. The incident velocity of the projectiles was measured using two pairs of infrared sensors located at the end of the barrel. New projectiles were employed for each impact test. The schematic and a photograph of the experimental set-up are shown in Fig. 5a,b, respectively.

A transparent safety chamber, with a metal frame and thick polycarbonate panels, was used to confine the end of the barrel and the target area, where the target specimen was fixed by a specific specimen support, see Fig. 6. The specimen support consisted of two main components: one component being the steel supporting plate which had a 70 mm × 70 mm cut-out and a thickness of 20 mm and the other component was the steel clamping plate, which had an opening of 70 mm × 70 mm and a thickness of 15 mm. These two components were connected and fastened using twelve 'M8' sized bolts.

A 3D DIC system was used to measure the deformation of the rear-face of the specimens during impact loading. Two 'Phantom Miro M/R/LC310' high-speed cameras, supplied by Vision research Phantom®, USA. These two cameras were separated from each other by 410 mm and located behind the composite specimens, with a working distance of 925 mm from the centre point of the target. A pair of identical 'Nikon' lenses with a fixed focal length of 50 mm, supplied by Nikon Ltd.®, UK, were used with these two

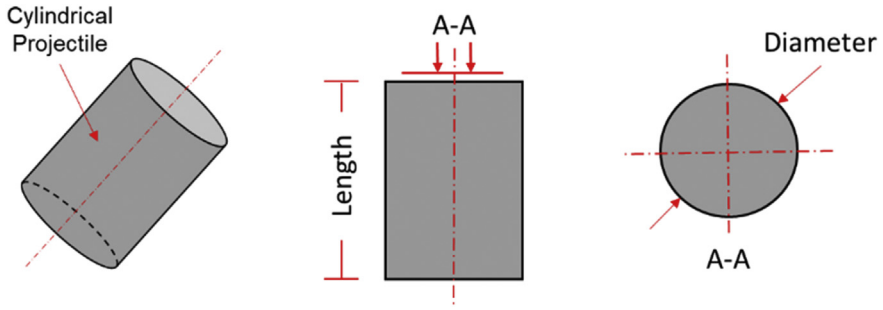

Fig. 2. The geometry of the gelatine and HDPE projectiles for the gas-gun experiments.

Table 1
Physical properties of the gelatine and HDPE projectiles [13–15].

Projectile	Density (g cm^{-3})	Mass (g)	Diameter (mm)	Length (mm)	Nominal hardness
Gelatine	1.06 ± 0.003	20 ± 0.5	23 ± 0.5	45 ± 0.5	Shore hardness A of 5–10
HDPE	0.95 ± 0.002	20 ± 0.5	23 ± 0.5	50 ± 0.5	Shore hardness D of 60–70

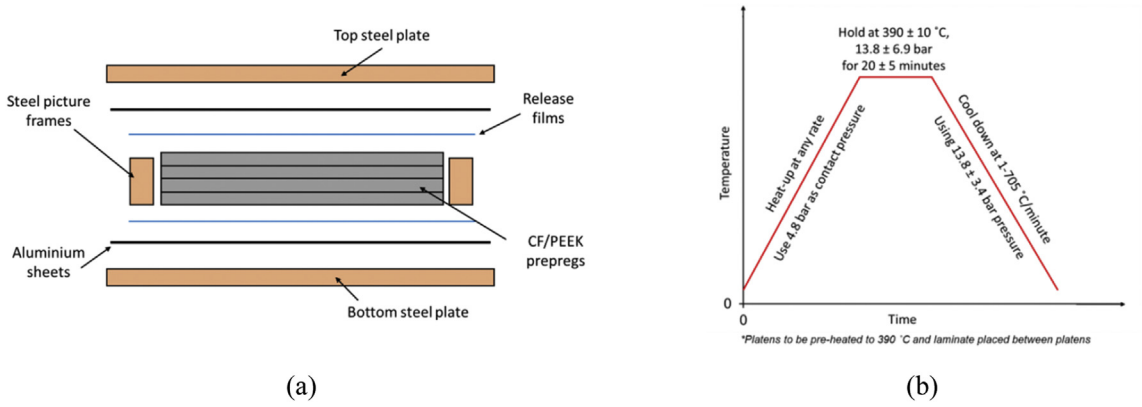

Fig. 3. Diagrams of (a) the consolidation jig and (b) the cure schedule for the CF/PEEK prepregs.

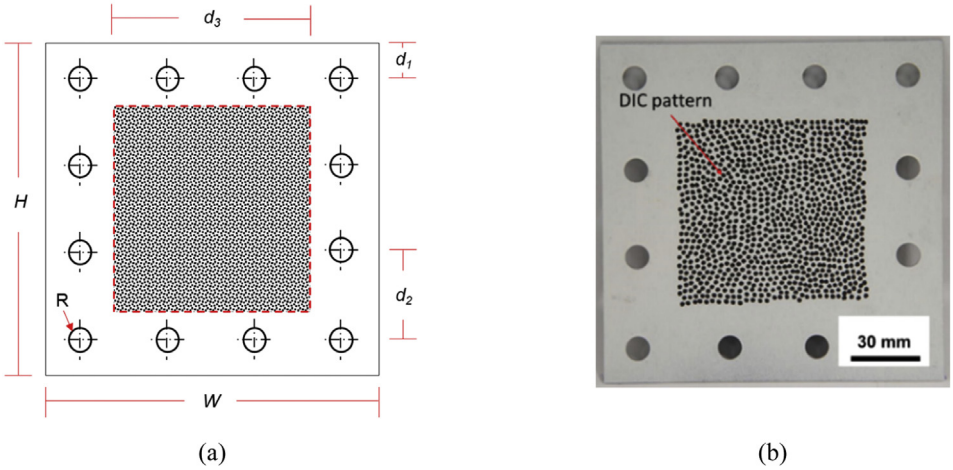

Fig. 4. Composite target test specimens: (a) schematic and (b) the pattern for the DIC.

Table 2
Dimensions of the CF/PEEK composite target test specimens.

Dimensions	W (mm)	H (mm)	d_1 (mm)	d_2 (mm)	d_3 (mm)	R (mm)
Values	140	140	16	36	70	5

cameras. During the tests, the recording rate of these two cameras was set as 40,000 frames per second and they were triggered simultaneously by the signal generated from the infrared sensors. To achieve the brightness required for the high-speed DIC system,

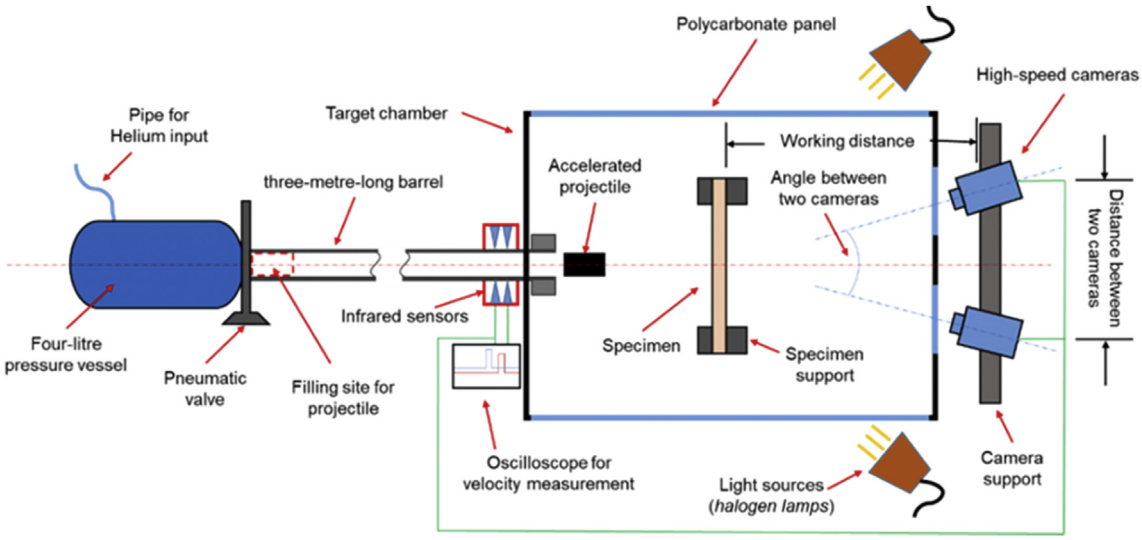

(a)

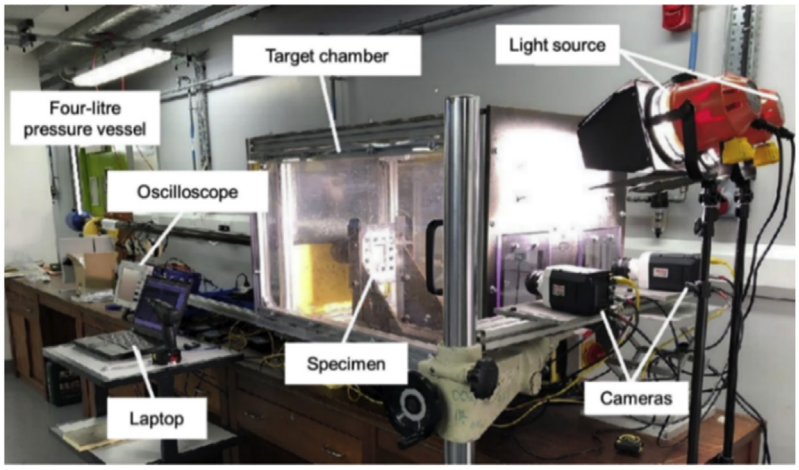

(b)

Fig. 5. Experimental set-up for the gas-gun impact experiments: (a) schematic and (b) photograph.

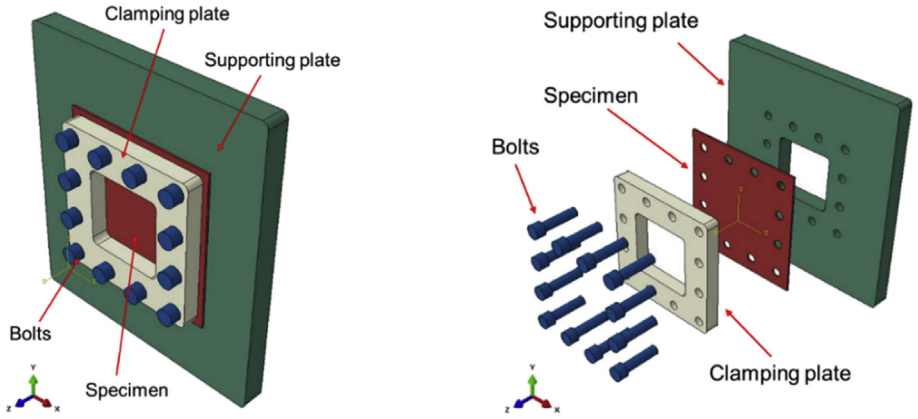

(a) (b)

Fig. 6. Specimen support: (a) assembled and (b) disassembled.

two bright light sources, which were only turned on a few seconds before the gas-gun was fired, were employed to illuminate the rear-surface of the composite specimens. The area of interest for the DIC measurement was 60 mm × 60 mm, which is slightly smaller than the DIC pattern area on the specimens.

4. Experimental procedure

In the gas-gun impact experiments, the impact energy is equal to the kinematic energy of the projectile, which can be calculated based on the mass and velocity of the projectile, and is given by:

$$E_k = \frac{1}{2} m v_0^2 \quad (1)$$

where E_k is the impact energy or the kinetic energy of the projectile and m and v_0 are the mass and the velocity at impact of the projectile, respectively. To study the effects on the composite from steadily increasing the impact energy levels, a given test specimen was successively impacted from a relatively low-energy level to a high-energy level by steadily increasing the impact velocity of the projectile.

To investigate the effects of projectile hardness, the gelatine projectiles and HDPE projectiles were employed to impact the CF/PEEK specimens at a similar energy level. For each case, three CF/PEEK specimens were tested. The test details for these experiments are summarised in Table 3.

After the impact tests had been undertaken, a visual inspection was conducted on the composite specimens and photographs were taken of the rear-surface of the post-impacted specimens. In general, the type of damage suffered by the composite panels could be categorised as: (a) no visible damage present, (b) cracking observed, (c) fracture having occurred, and (d) perforation (i.e. penetration of the projectile through the specimen) also having occurred. The main difference between type (b) cracking and type (c) fracture is whether there was fibre breakage observed. For type (b) cracking, this was defined as when cracks were only observed in the matrix. However, for type (c) fracture, fibre failure was also observed. Schematics of these descriptions for the damage of the post-impact results for the composite specimens are shown in Fig. 7.

5. Results and discussion

5.1. Projectile deformation

The deformation history of the gelatine projectile obtained from the experimental studies, for a kinetic energy of 37 J (velocity 61 m.s^{-1}) is shown in Fig. 8. The experimental results show that, at the beginning of the impact event (i.e. t = 0.0 ms), the shape of the gelatine projectile was well preserved, which ensured that the gelatine projectile impacted the centre of the specimen and then deformed symmetrically. After the initial contact with the composite specimen (i.e. t = 0.2–0.3 ms), the front of the gelatine projectile started to deform and flow to the periphery of the composite specimen. At a later stage of the impact event (i.e. t = 0.6 ms), most of the gelatine projectile has deformed, flowed and spread over the surface of the composite specimen. This confirmed that the gelatine projectile can clearly be seen to be flowing freely after impact.

5.2. Major strain

Fig. 9 shows two example of dynamic major strain maps obtained from the 3D DIC system, used to measure the deformation of the rear-face of the specimens, during impact loading. Fig. 9a shows an example of a major strain map obtained from the CF/PEEK specimen impacted with a gelatine projectile for a kinetic energy of 37 J (i.e. an impact velocity of 61 m.s^{-1}). Fig. 9b shows an example of a major strain map for a CF/PEEK specimen impacted with a HDPE projectile for a kinetic energy of 34 J (i.e. an impact velocity of 58 m.s^{-1}).

Based on the major strain history, the evolution of the major strains along the horizontal mid-section, during the loading and unloading process, were also extracted, see Fig. 10, for the gelatine-impacted and the HDPE-impacted CF/PEEK specimens, see Fig. 10a,b respectively, where the solid black line indicates the horizontal mid-section of the tested specimens.

5.3. Out-of-plane (OOP) displacement

The OOP of the composite specimens during the soft and hard impact experiments was also recorded using the 3D DIC system and examples are shown in Fig. 11. The OOP displacement contours, corresponding to different times during the impact test, were extracted from the DIC results obtained from the gelatine-impacted and HDPE-impacted composite specimens, see Fig. 11a,b respectively.

Similarly, the OOP displacements along the horizontal mid-section, during the loading and unloading of the specimen, were also obtained based on the contour maps of the OOP displacement obtained from the gelatine-impacted and HDPE-impacted CF/PEEK specimens, see Fig. 12a,b, respectively. The maximum OOP displacement for the gelatine-impacted and HDPE-impacted composite specimens is 3.9 ± 3% mm and 4.3 ± 3% mm, respectively.

5.4. Post-impact status

Visual inspections were conducted on the post-impacted CF/PEEK specimens. The gelatine projectile left no damage on the front and rear surface of the specimen. The HDPE projectile was undeformed after impact and left a faint ring mark on the front face. However, a fracture band ring of damage was clearly visible on the rear surface. Fig. 13 shows photographs taken of the rear surfaces of the three gelatine-impacted and three HDPE-impacted CF/PEEK specimens. It is clearly evident that all the gelatine-impacted specimens exhibited no damage on the rear surface and the HDPE-impacted specimens clearly have circular fracture bands visible on the rear surface. This illustrates that good consistency was obtained from the gas-gun experiments.

Fig. 14 shows a comparison of the post-impact behaviour of the gelatine-impacted and HDPE-impacted CF/PEEK specimens, with magnified images of the central area also shown. In Fig. 14a it may be seen that the gelatine-impacted CF/PEEK specimen did not show any visible damage whilst the HDPE-impacted CF/PEEK specimen shows significant damage on the rear surface, see Fig. 14b.

The HDPE-impacted CF/PEEK specimen exhibited a characteristic circular fracture band on the rear surface, as shown in Fig. 14b. Thus, at very similar impact energies, this reveals that the CF/PEEK

Table 3
Testing configurations for investigating the effects of projectile hardness.

Tests	Projectile	Matrix system	Projectile mass (g)	Velocity (m.s^{-1})	Impact energies (J)
GCP-I	Gelatine	PEEK	20 ± 1	61 ± 5%	37 ± 3%
HCP-I	HDPE	PEEK	20 ± 1	58 ± 5%	34 ± 3%

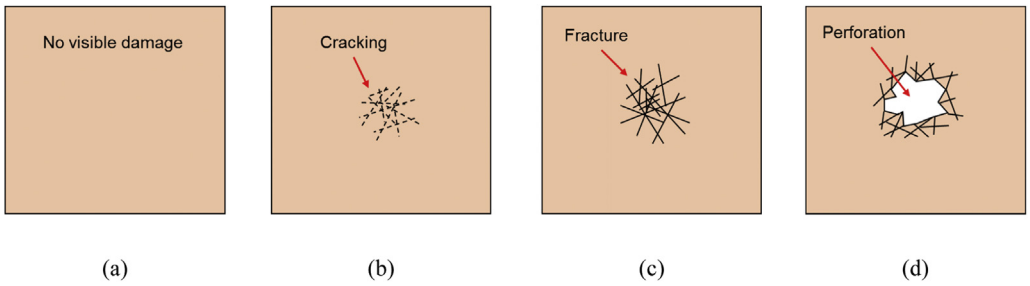

Fig. 7. Schematic of types of damage in post-impact specimens: (a) no visible damage, (b) cracking, (c) fracture, and (d) perforation.

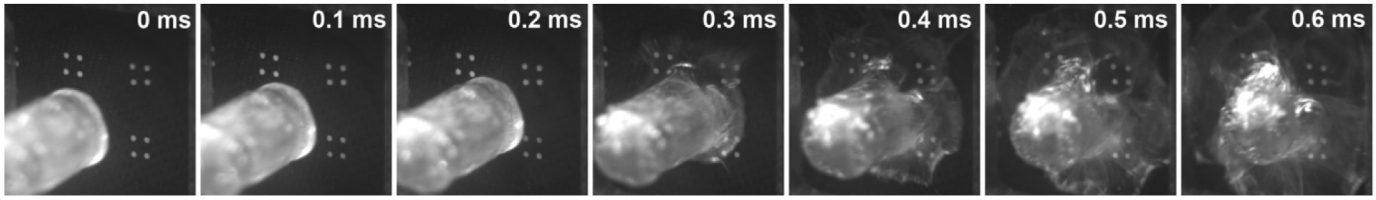

Fig. 8. High-speed photographic time-sequence of the impact of a gelatine projectile at 37 J (velocity 61 ± 5% m.s^{-1}).

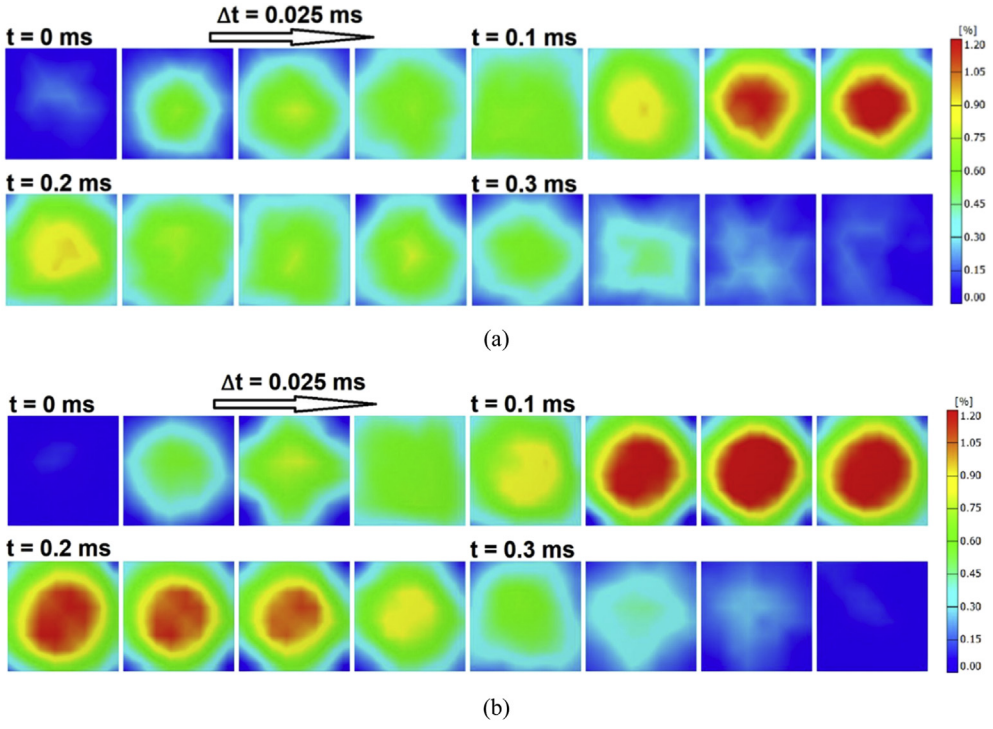

Fig. 9. The dynamic major strain maps: (a) the CF/PEEK specimen impacted with a gelatine projectile at 37 J (impact velocity 61 ± 5% m.s^{-1}) and (b) the CF/PEEK specimen impacted with a HDPE projectile at 34 J (impact velocity 58 ± 5% m.s^{-1}).

composite is more vulnerable to the HDPE projectile which has a relatively high hardness.

5.5. Ultrasonic C-scan

A portable ultrasonic scan system was used to examine all the impacted specimens before and after the soft-projectile impact experiments. Prior to the impact experiments, the ultrasonic scanning inspection was performed on all the composite specimens to ensure that no damage was caused during manufacture, transportation and storage. The relevant ultrasonic scanning images, shown in Fig. 15, reveal that no delamination occurred in the gelatine-impacted specimens, whilst very clear delamination is observed in the HDPE-impacted composite specimens. These C-scan maps show delamination as a function of the depth through the thickness of the specimen, where the red colour is representative of the front (impacted) surface and blue colour is representative of the rear (non-impacted) surface of the specimen.

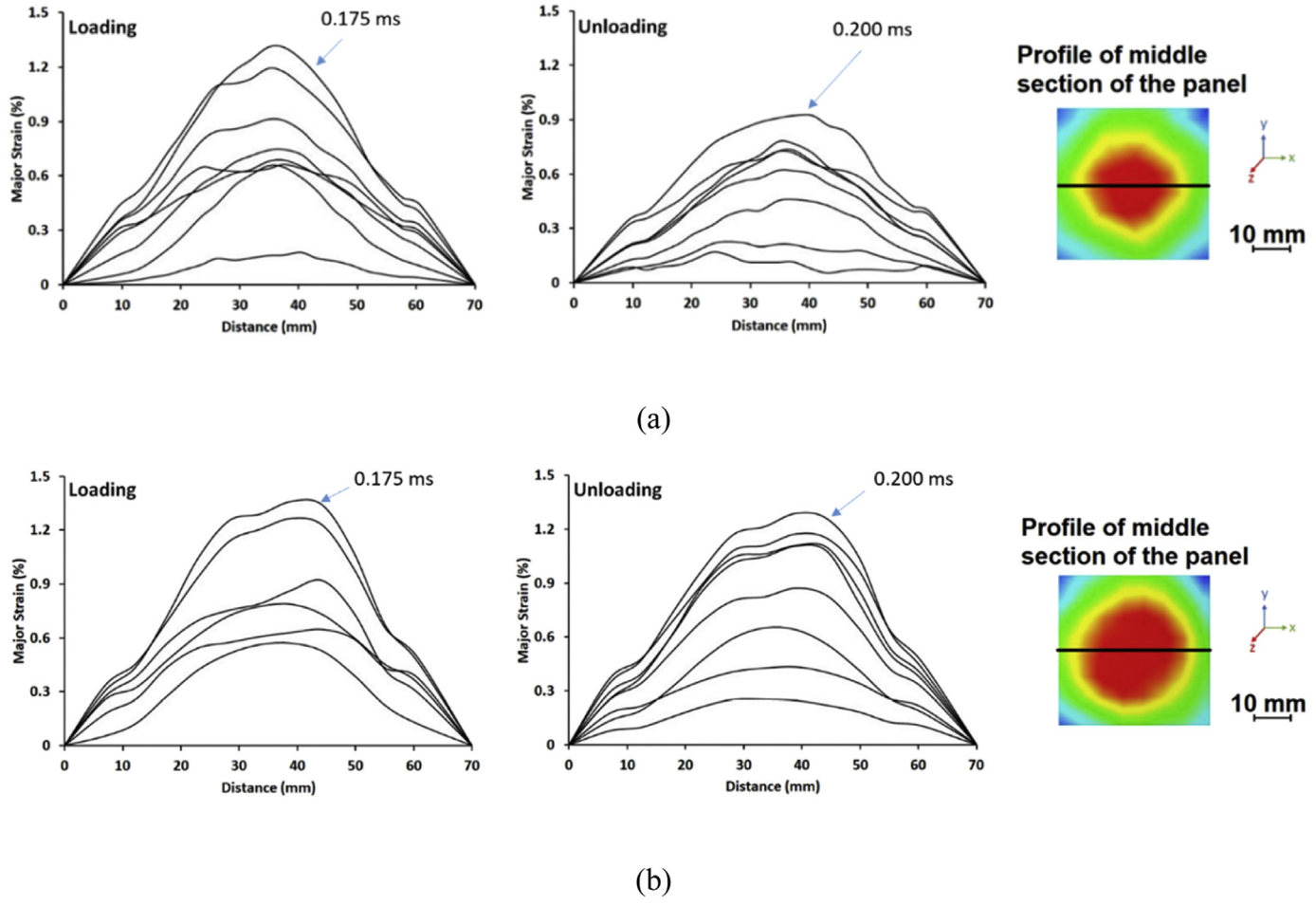

Fig. 10. The evolution of the major strain during the specimen being loaded and then unloading: (a) the CF/PEEK specimen impacted with a gelatine projectile at 37 J (impact velocity 61 ± 5% m.s^{-1}) and (b) the CF/PEEK specimen impacted with a HDPE projectile at 34 J (impact velocity 58 ± 5% m.s^{-1}). The inset photograph shows a horizontal solid line where the profile section is taken.

5.6. Summary of results

For the relatively hard HDPE projectile impacting on the CF/PEEK sample, the HDPE projectile was undeformed after impact but the projectile left a distinctive mark on the front surface of the composite specimen and a circular fracture on the rear-surface of the specimen was present, as explained above. Experimental results obtained from the HDPE-impacted CF/PEEK specimen (for an impact energy of 34 J) are compared with the gelatine-impacted CF/PEEK specimen (for an impact energy of 37 J) in Table 4. By comparing the results for 'Test GCP-1' and 'Test HCP-1', it can be seen that employing the relatively hard HDPE projectile leads to (a) a similar but slightly larger value of the major strain and larger maximum OOP displacement for the CF/PEEK composite specimen, (b) far more major damage being suffered by the specimen upon being struck by the HDPE projectile.

5.7. Analysis and discussion

By comparing the results, it may be seen that employing the relatively hard HDPE projectile leads to: (a) a slightly increased maximum OOP displacement and, very significantly, (b) far more major damage being suffered by the test specimen upon being struck by the HDPE projectile. To explain these phenomena, schematics of the impact events on the CF/PEEK test specimens, subjected to an impact by both the relatively soft gelatine and the hard HDPE projectiles, are illustrated in Fig. 16.

Due its relatively low hardness, the soft gelatine projectile will tend to undergo considerable deformation after it has made initial contact with the target test specimen, which will lead to flow of the gelatine as shown schematically in Fig. 16a and as visible in Fig. 8. Subsequently, the deformed gelatine projectile has a larger contact area on the impacted face of the composite. This will reduce the average contact pressure caused by the impact loading, as given by:

$$P_c = \frac{F}{A_c} \tag{2}$$

where F is the impact load and P_c and A_c are the average contact pressure and contact area between the projectile and specimen, respectively. The maximum central out-of-plane (OOP) displacement on the rear surface of the composite specimen is noted to be slightly less for the gelatine projectile. This is due to the increase in the contact area, for the gelatine impact, due to flow of the soft gelatine. Notable in the schematic in Fig. 16b, for the HDPE projectile, is that the rear face deformation is slightly flattened early on in the deformation process, when compared with Fig. 15a for the gelatine projectile. The HDPE projectile deformed much less than the gelatine projectile and the contact area can be considered to be virtually constant during the impact event. Furthermore, the rounded edge of the relatively rigid HDPE projectile leads to a localised deformation in the composite specimens, which resulted in a stress concentration in this area particularly on the rear surface. This effect leads to more localised damage on the rear surface the

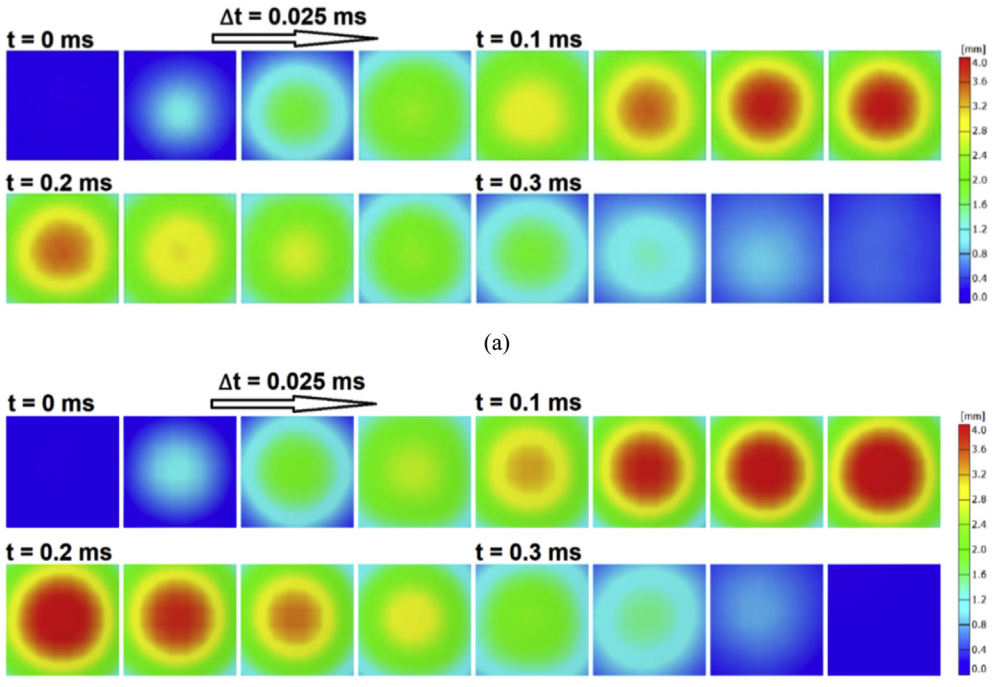

Fig. 11. The OOP displacement contours: (a) the CF/PEEK specimen impacted with a gelatine projectile at 37 J (impact velocity 61 ± 5% m.s^{-1}) and (b) the CF/PEEK specimen impacted with a HDPE projectile at 34 J (impact velocity 58 ± 5% m.s^{-1}).

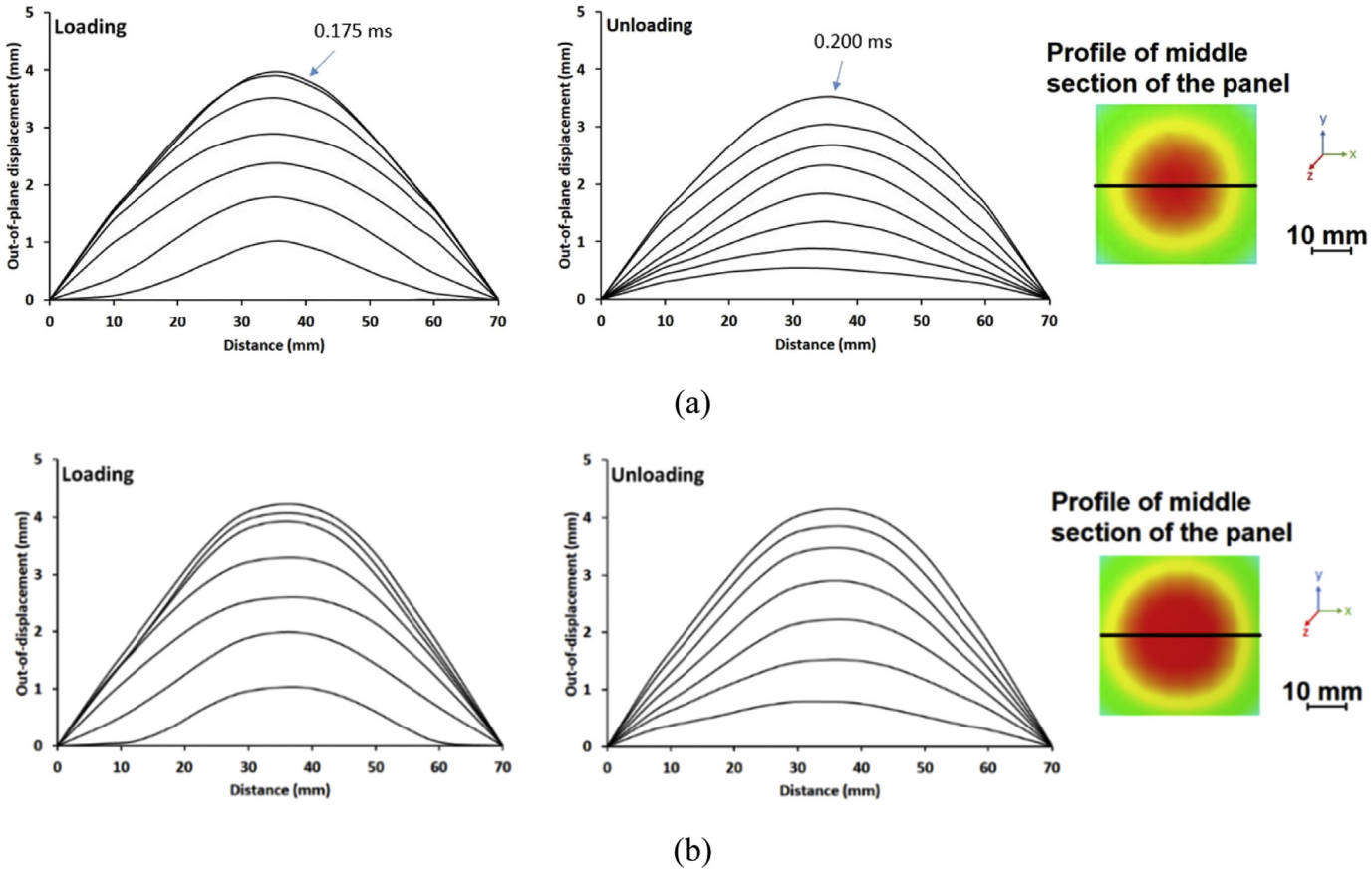

Fig. 12. The evolution of the OOP displacement profiles (in intervals of 0.025 ms) during loading and unloading: (a) the CF/PEEK specimen impacted with a gelatine projectile at 37 J (61 ± 5% m.s^{-1}) and (b) the CF/PEEK specimen impacted with a HDPE projectile at 34 J (58 ± 5% m.s^{-1}). The inset photograph shows a horizontal solid line where the profile section is taken.

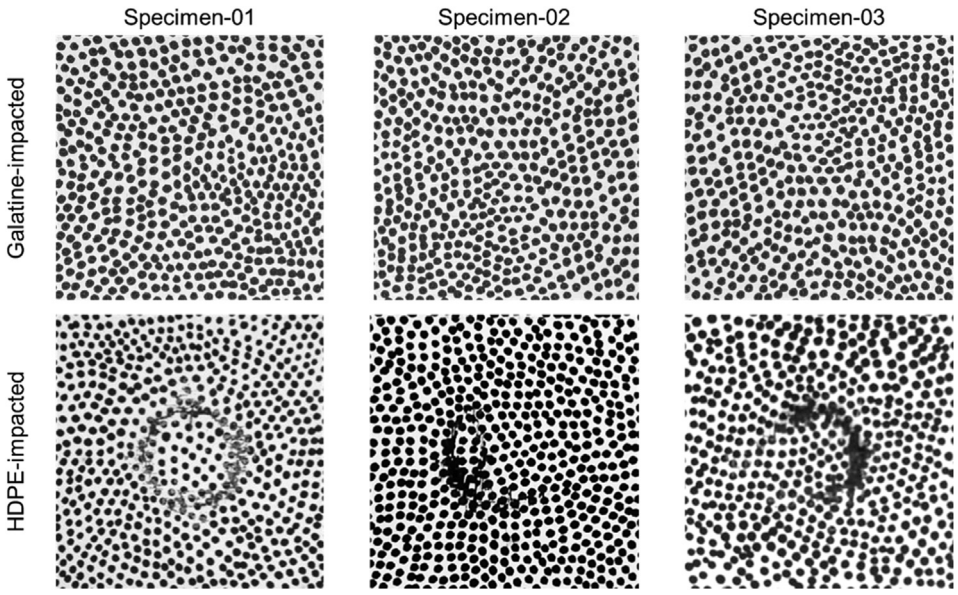

Fig. 13. Photographs of the rear surfaces of the gelatine-impacted and HDPE-impacted CF/PEEK specimens.

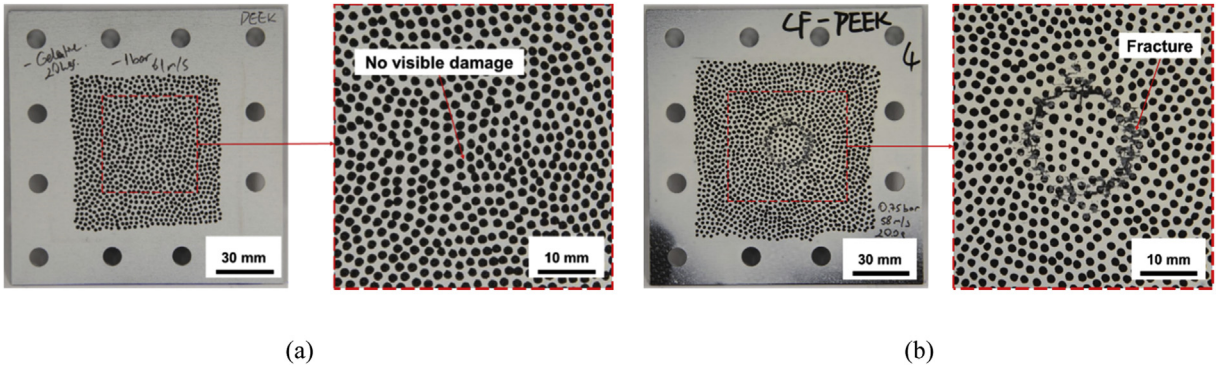

Fig. 14. Rear surfaces of the tested specimens: (a) the specimen impacted by a gelatine projectile with an energy of 37 J and (b) the specimen impacted by a HDPE projectile with an energy of 34 J.

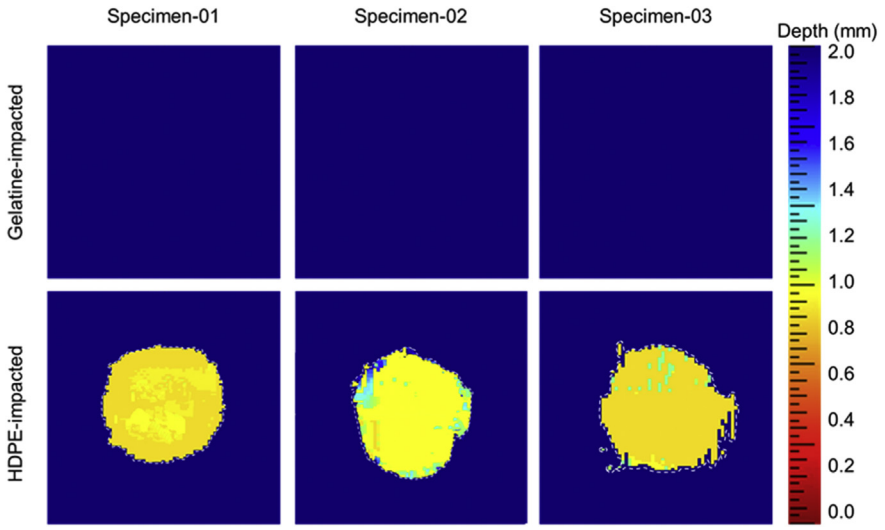

Fig. 15. Ultrasonic scanning images obtained from the gelatine-impacted and the HDPE-impacted CF/PEEK specimens.

Table 4
Summary of results for the CF/PEEK specimens after impact by the gelatine or the HDPE projectile.

Test	Projectiles	Velocities ($m.s^{-1}$)	Energies (J)	Post-impact damage	Maximum major strain	Maximum OOP displacement (mm)
GCP-I	Gelatine	61 ± 5%	37 ± 3%	Type (a) in Fig. 7 - no visible damage	0.013 ± 3%	3.9 ± 3%
HCP-I	HDPE	58 ± 5%	34 ± 3%	Type (c) in Fig. 7 - fracture	0.014 ± 3%	4.3 ± 3%

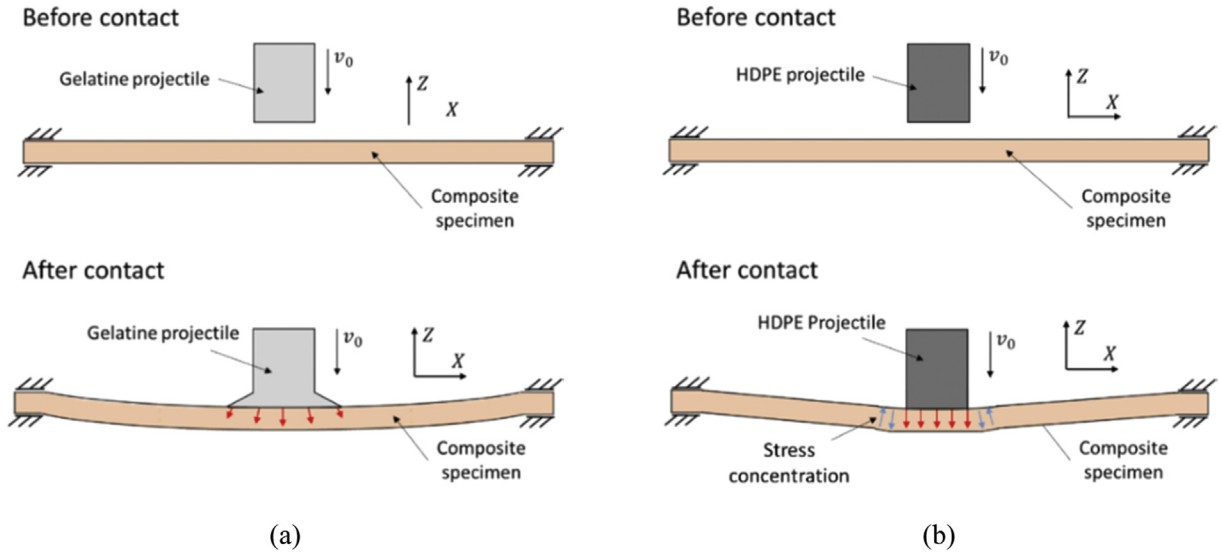

Fig. 16. Schematics of the impact test for different types of projectile: (a) a specimen impacted by a relatively soft gelatine projectile and (b) a specimen impacted by a relatively hard HDPE projectile.

composite test specimens for the HDPE projectile compared with the gelatine projectile.

6. Conclusions

This paper has focussed on experimental investigations of the effects of projectile hardness on the impact response of fibre-reinforced composites. Gas-gun experiments were performed on woven carbon-fibre reinforced poly (ether-ether ketone) (CF/PEEK) composite specimens. To investigate the effects of projectile hardness on the impact response of composite laminates, soft gelatine projectiles and hard high-density polyethylene (HDPE) projectiles were prepared and used to impact the (CF/PEEK) composite specimens. A Digital Image Correlation (DIC) system was used to record the deformation of the composite specimens during the experiments. A high-speed camera was also employed to record the deformation of the projectiles during the impact process. The high-speed camera recorded frames which showed that the gelatine projectiles behaved like a viscoelastic fluid upon impacting the CF/PEEK specimens. The DIC results demonstrated that the composite specimens impacted by the hard HDPE projectiles underwent similar, but slightly larger, values of the major strain and the out-of-plane displacement than the composite specimens impacted by the soft gelatine projectiles. In addition, the post-impact analyses, including both the visual inspection and ultrasonic C-scan results, demonstrated that the CF/PEEK woven composites were more vulnerable to the relatively hard HDPE projectile compared with the relatively soft gelatine projectile. This was mainly attributed to the higher contact pressures generated by the HDPE projectile, particularly around the edge of the contact area. This research is very relevant to the commercial aircraft industry, as carbon-fibre reinforced composites, which are finding increasing application, can experience damage from birds and relatively harder particles, e.g. hail and runway debris.

Conflicts of interest

The authors declare that there is no conflicts of interest.

Acknowledgements

The strong support from the Aviation Industry Corporation of China (AVIC) Manufacturing Technology Institute (MTI), the First Aircraft Institute (FAI) and the Aircraft Strength Research Institute (ASRI) for this funded research is much appreciated. The research was performed at the AVIC Centre for Structural Design and Manufacture at Imperial College London, UK.

References

[1] A. Kelly, Composite materials after seventy years, J. Mater. Sci. 41 (2006) 905–912.
[2] B. Krishan, K.K. Chawla, Composite Materials: Science and Engineering, Springer Science & Business Media, 2012.
[3] H. Liu, B.G. Falzon, S. Li, W. Tan, J. Liu, H. Chai, B.R.K. Blackman, J.P. Dear, Compressive failure of woven fabric reinforced thermoplastic composites with an open-hole: an experimental and numerical study, Compos. Struct. 213 (2019) 108–117.
[4] B. Vieille, V.M. Casado, C. Bouvet, About the impact behavior of woven-ply carbon fiber-reinforced thermoplastic- and thermosetting-composites: a comparative study, Compos. Struct. 101 (2013) 9–21.
[5] E. Panettieri, D. Fanteria, M. Montemurro, C. Froustey, Low-velocity impact tests on carbon/epoxy composite laminates: a benchmark study, Compos. Part B Eng. 107 (2016) 9–21.
[6] H. Liu, B.G. Falzon, W. Tan, Experimental and numerical studies on the impact response of damage-tolerant hybrid unidirectional/woven carbon-fibre reinforced composite laminates, Compos. Part B Eng. 136 (2018) 101–118.
[7] H. Liu, B.G. Falzon, W. Tan, Predicting the Compression-After-Impact (CAI) strength of damage-tolerant hybrid unidirectional/woven carbon-fibre reinforced composite laminates, Compos. Part A Appl. Sci. Manuf. 105 (2018) 189–202.
[8] J. Liu, H. Liu, C. Kaboglu, X. Kong, Y. Ding, H. Chai, B.R.K. Blackman, A.J. Kinloch, J.P. Dear, The impact performance of woven-fabric thermoplastic and thermoset composites subjected to high-velocity soft and hard impact loading,

Appl. Compos. Mater. (2019), https://doi.org/10.1007/s10443-019-09786-2 (Accepted on 27/08/2019).
[9] S.A. Kalam, V.K. Rayavarapu, R.J. Ginka, Impact behaviour of soft body projectiles, J. Inst. Eng. Ser. C 99 (2018) 33–44.
[10] J.P. Hou, C. Ruiz, Soft body impact on laminated composite materials, Compos. Part A Appl. Sci. Manuf. 38 (2007) 505–515.
[11] J. Zhou, J. Liu, X. Zhang, Y. Yan, L. Jiang, I. Mohagheghian, J.P. Dear, M.N. Charalambides, Experimental and numerical investigation of high velocity soft impact loading on aircraft materials, Aerosp. Sci. Technol. 90 (2019) 44–58.
[12] H. Kim, K.T. Kedward, Modeling hail ice impacts and predicting impact damage initiation in composite structures, AIAA J. 38 (2012) 1278–1288.
[13] F. Allaeys, G. Luyckx, W. Van Paepegem, J. Degrieck, Numerical and experimental investigation of the shock and steady state pressures in the bird material during bird strike, Int. J. Impact Eng. 107 (2017) 12–22.
[14] M.A. Lavoie, A. Gakwaya, M.N. Ensan, D.G. Zimcik, D. Nandlall, Bird's substitute tests results and evaluation of available numerical methods, Int. J. Impact Eng. 36 (2009) 1276–1287.
[15] Overview of Materials for High Density Polyethylene (HDPE), MatWeb Material Property data, 2018. http://www.matweb.com/search/PropertySearch.aspx.